Catalysis Today 172 (2011) 95–102

Contents lists available at ScienceDirect

Catalysis Today

journal homepage: www.elsevier.com/locate/cattod

Total CO oxidation over Fe-containing Au/HMS catalysts: Effects of gold loading and catalyst pretreatment

R.E. Ramírez-Garza[a], B. Pawelec[b], T.A. Zepeda[c], A. Martínez-Hernández[a,*]

[a] Facultad de Ciencias Químicas, Universidad Autónoma de Nuevo León, Ciudad Universitaria, C.P. 66400, N.L., Mexico
[b] Instituto de Catálisis y Petroleoquímica, CSIC, c/Marie Curie 2, Cantoblanco, 28049 Madrid, Spain
[c] Centro de Nanociencias y Nanotecnología – UNAM, Km. 107 Carretera Tijuana-Ensenada, C.P. 22800, Ensenada, B.C., Mexico

ARTICLE INFO

Article history:
Received 30 November 2010
Received in revised form 2 February 2011
Accepted 18 February 2011
Available online 12 April 2011

Keywords:
CO oxidation
Mesoporous silica
Fe–HMS
Au catalysts
Cationic gold

ABSTRACT

In this work we report the effects of catalyst pretreatment (oxidation versus reduction) and gold loading on the catalytic response of Au/HMS–Fe catalysts for the CO oxidation reaction. Hexagonal mesoporous silica (HMS) substrates modified with Fe^{3+} ions (Si/Fe molar ratio of 40) were prepared via a neutral S^0I^0 templating route employing one-pot synthesis, whereas the supported gold catalysts with different Au concentrations were prepared by the deposition–precipitation method. The activity was measured by temperature-programmed reaction tests in the 20–400 °C range, and the catalysts were characterized by different techniques (S_{BET}, XRD, H_2-TPR, DRS UV–vis, XPS and DRIFTS). It was found that catalytic activity was a function of Au-loading being the most active the catalyst with the highest Au loading (5.1 wt%). The light-off curves showed a positive effect on the catalytic activity by a reduction treatment prior to performing the catalytic reaction. From DRIFTS study of co-adsorption of CO and O_2, it was concluded that the cationic gold species were the active phase in CO oxidation reaction. From the discussion of activity and characterization results it is proposed a reaction path where CO oxidation reaction takes place at the interface between gold cationic species and the iron sites.

1. Introduction

In the beginnings of the last century and until the sixties, the Au metal was known as catalytically inactive because it was used in a macroscopic form (wire, foils, etc.) [1]. Bond and Sermon [2,3] found that gold could be used in several reactions like hydrogenation of olefins, unsaturated molecules and hydrocracking reactions, among others. After such findings, Haruta et al. discovered that supported gold catalysts prepared by the coprecipitation method are highly active for CO oxidation which can reach a 100% of conversion at temperatures as low as −70 °C [4]. Since Haruta's discovery, there has been intense research activity concerning the use of gold as catalyst. It has been shown that the performance of gold catalysis depends on many factors, among which the synthesis method [5–9], particle size and treatments of the catalysts before reaction [10–13] remain prominent. These factors lead to important changes into the gold species, which are responsible for the activity of the catalysts. It has been suggested that the change of the particle size is linked with the type of treatment that also leads to the formation of species like metallic gold (Au^0), and partially ($Au^{\delta+}$) or fully oxidized gold (Au^{+3}) species. Changes in gold species have been related with the activity of catalysts in CO oxidation, although this matter is still under debate. Some authors have found that Au^0 species are responsible for activity [14,15] whereas others have identified the concentration of Au^{+3} [16] or the relative proportion Au^0/Au^{+3} as the catalytically active species in the target reaction [17,18]. Also, some reports stated that the nature of active gold species depends on the type of support used and pretreatment prior to reaction, enhancing in this way the catalyst performance [19,20]. Thus, supported gold catalysts over silicon dioxide are well known by their low activity compared with those supported in reducible oxides like Fe_2O_3, TiO_2, ZrO_2, Y_2O_3, La_2O_3 [19–23]. The addition of a reducible oxide like titanium oxide to non-reducible oxides results in an enhancement of gold dispersion avoiding sinterization [24]. Hexagonal mesoporous silica (HMS) synthesized by Tanev and Pinnavaia [25] presented a good thermal and hydrothermal stability, homogeneous meso-porosity and high specific surface area. As these properties favor the dispersion of metals, the HMS system is an excellent support candidate [26,27].

The deactivation of supported gold catalysts with time on-stream is an important factor that could hamper the industrial development of Au-based catalysts. However, the mechanism of catalyst deactivation and regeneration are still under debate [28]. Gold aggregation is one of the most important issues that leads to catalysis deactivation due its low melting point when it exists as

* Corresponding author. Tel.: +52 8183753429.
E-mail addresses: amartinezh@mail.uanl.mx, angeloiiia@gmail.com (A. Martínez-Hernández).

0920-5861/$ – see front matter © 2011 Elsevier B.V. All rights reserved.
doi:10.1016/j.cattod.2011.02.067

Table 1
Textural properties and Au loading of the pure support and fresh Au/HMS–Fe catalysts.

Sample	Au[a] (wt%)	S_{BET}[b] (m^2/g)	NS_{BET}[b]
HMS–Fe	–	699	–
0.4%Au/HMS–Fe	0.4	721	1.0
1.2%Au/HMS–Fe	1.2	750	1.1
2.0%Au/HMS–Fe	2.0	683	1.0
3.1%Au/HMS–Fe	3.1	485	0.7
5.1%Au/HMS–Fe	5.1	469	0.7

[a] Au loading determined by ICP technique.
[b] As determined by N_2 physisorption at 196 °C: S_{BET}: specific BET surface area; NS_{BET}: normalized S_{BET} calculated from equation $NS_{BET} = (S_{BET}$ of oxide catalyst/$[(1-y) \times S_{BET}$ of support$]$), where y is the Au loading determined by chemical analysis (ICP).

nanoparticles (<10 nm) [10]. Moreover, the possible explanations proposed in literature for deactivation of supported gold catalysts during CO oxidation involve blockage of interfacial sites by water, deposition of "carbon species", elimination of surface hydroxyl groups ([29] and refs. therein) and reduction of Au cationic species [30]. Moreover, based on IR studies, evidence was provided that CO and CO_2 competed for adsorption on the same site on Au surfaces leading to catalyst deactivation [31–33]. On the contrary, recently, DRIFTS study on the mode of Au/TiO_2 catalyst deactivation point out to non-competitive adsorption of CO and O_2 on the surface of Au species [28].

In line with this, the present work was undertaken with the aim to determine the effect of pre-treatment (oxidation versus reduction) on the catalytic response of gold catalysts supported on a HMS–Fe substrate in reaction of total CO oxidation. In particular, the nature of gold species for different metal loadings and its influence on the activity and catalyst deactivation were investigated.

2. Experimental

2.1. Synthesis of support and catalysts

The support HMS–Fe was synthesized using a method described by Castaño et al. [34]. The gold catalysts were prepared by the deposition–precipitation method, using solutions of $HAuCl_4 \cdot 3H_2O$ (Fisher 99%) as gold precursor whose metal concentrations were appropriately selected to obtain metal loadings in the range 0.4–5.1 wt%. The gold solution was slowly added with a moderate stirring to a solution containing the support suspended in deionized water whereas the pH of resultant slurry was kept fixed at 9 using an ammonium hydroxide solution (0.07 M). The final slurry was filtered and washed with deionized water using ten times the volume reached in the final solution. The solid was dried at 110 °C for 10 h and calcined at 400 °C for 4 h. Table 1 shows the gold loading and nomenclature of the catalysts.

2.2. Catalytic activity measurements

The activity measurements for CO oxidation over Au catalysts were carried out in a quartz tubular microreactor using a total flow of 100 cm^3/min and 300 mg of catalyst (GHSV ~3156 h^{-1}). The reactor feed composition was of 2% CO, 2% of O_2 and 96% of N_2. Reactor temperature was raised from room temperature up to 400 °C using a heating rate of 3 °C/min. The composition of the reactor inlet and exit streams was determined by on-line gas chromatograph (Shimadzu 15A) equipped with a molecular sieve 5A packed column. Catalytic activity was calculated according to equation: $X_{CO} = (C_{COi} - C_{COf})/C_{COi} \times 100$, where C_{COi} is the concentration of CO in the feed stream and C_{COf} is the CO concentration at the reactor outlet. Before reaction, the catalysts were pretreated under oxidative or reductive atmosphere in order to evaluate the influence of pretreatments on the catalytic activity of Au–HMS–Fe catalysts. The oxidation pretreatment consisted in passing through the reactor 50 cm^3/min of dry air keeping the reactor temperature at 400 °C for 1 h. The reduction pretreatment consisted in passing through the reactor a mixture of 10% H_2 in N_2 balance (total flow of 100 cm^3/min) while the reactor temperature was kept at 300 °C for 0.5 h.

2.3. Characterization methods

The gold loading of the fresh catalysts was determined by Inductively Coupled Plasma Atomic Emission Spectroscopy (ICP-AES) using a Perkin Elmer Optima 3300DV equipment. Specific BET surface areas of the HMS–Fe substrate and fresh Au/HMS–Fe catalysts were evaluated by N_2 adsorption–desorption isotherms at −196 °C. The normalized S_{BET} was calculated using the equation $NS_{BET} = (S_{BET}$ oxide catalyst/$[(1-y) \times S_{BET}$ of support$]$), where y is the Au loading determined by chemical analysis (ICP).

The pure support and calcined catalysts were characterized by powder X-ray diffractometry according to the step-scanning procedure (step size 0.02°; 0.5 s) with a computerized Philips X'Pert spectrometer using CuKα radiation ($\lambda = 0.15406$ nm). DRS UV–vis spectra were taken using a Praying Mantis accessory with the use of a high reaction temperature chamber (HRTC) from Harrick, attached to a Cary 5E spectrometer (Varian). X-ray photoelectron spectra were acquired with a VG Escalab 200R spectrometer equipped with a hemispherical electron analyzer operating in the constant pass-energy mode ($E_{pass} = 20$ eV) and an Mg Kα ($h\nu = 1253.6$ eV) radiation. The binding energy (BE) of Au 4f, Fe $2p_{3/2}$ and O 1*s* were referenced to the Si 2p peak at 103.4 eV. Surface atomic ratios were calculated from the peak area ratios normalized by the corresponding atomic sensitivity factors. H_2-TPR experiments were performed in home-made flow equipment. Basically, a sample of 30 mg of catalyst was reduced under a flow of 25 cm^3/min of a mixture of 5% H_2/Ar through the reactor. The temperature of the reactor was raised from room temperature up to 1000 °C at a heating rate of 10 °C/min. Hydrogen consumption was measured by mean of a thermal conductivity detector (TCD). DRIFT analysis was carried out at room temperature using a Nicolet 5ZDX Fourier transform spectrophotometer equipped with a Harrick diffuse reflectance accessory (HVC-DRP cell). Calcined sample (ca. 50 mg) was thermally treated in He at 300 °C for 0.5 h prior to exposition at room temperature to a 4% CO in air mixture for 0.5 h. A similar DRIFTS study was performed on the sample pre-treated by oxidation (400 °C for 1 h) or reduction (300 °C for 0.5 h).

3. Results and discussion

3.1. Catalytic activity

Au/HMS–Fe catalysts were tested in the CO oxidation at temperatures ranging from room temperature to 400 °C with the aim of studying the effects of catalyst pre-treatment and Au loading on the catalyst activity in this reaction. Before reaction, the catalyst was activated by oxidation in air at 400 °C for 1 h or by reduction in 10%H_2/N_2 mixture at 300 °C for 0.5 h. It is well known that 100% of CO conversion is thermodynamically favoured at temperatures below room temperature. In the absence of any treatment, it was observed that the light-off curve of the catalyst with the highest Au loading (5.1 wt%) begins at room temperature with a 10% of CO conversion, which is quite far from the thermodynamic equilibrium, and reached the equilibrium conversion at reaction temperatures above 200 °C (data not shown here).

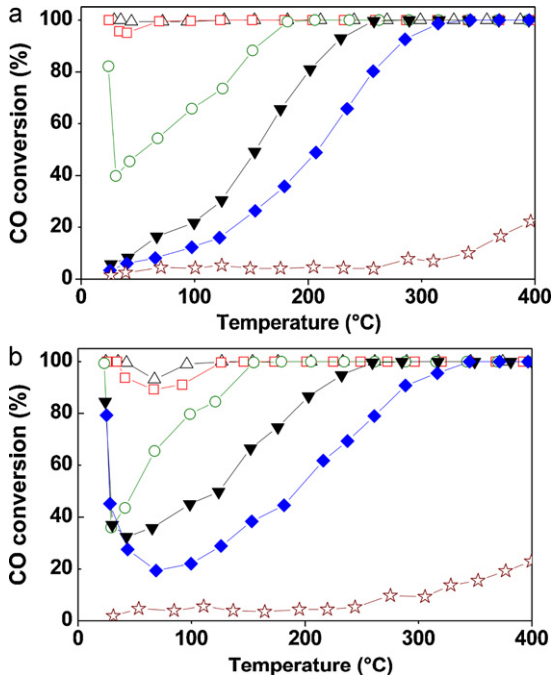

Fig. 1. CO oxidation over Au/HMS–Fe catalysts (T = 25–400 °C; P = 1 bar) activated by oxidation (a) and reduction (b): pure HMS–Fe (☆); 0.4%Au/HMS–Fe (⧫); 1.2%Au/HMS–Fe (▽); 2.0%Au/HMS–Fe (◯); 3.1%Au/HMS–Fe (□); 5.1%Au/HMS–Fe (△).

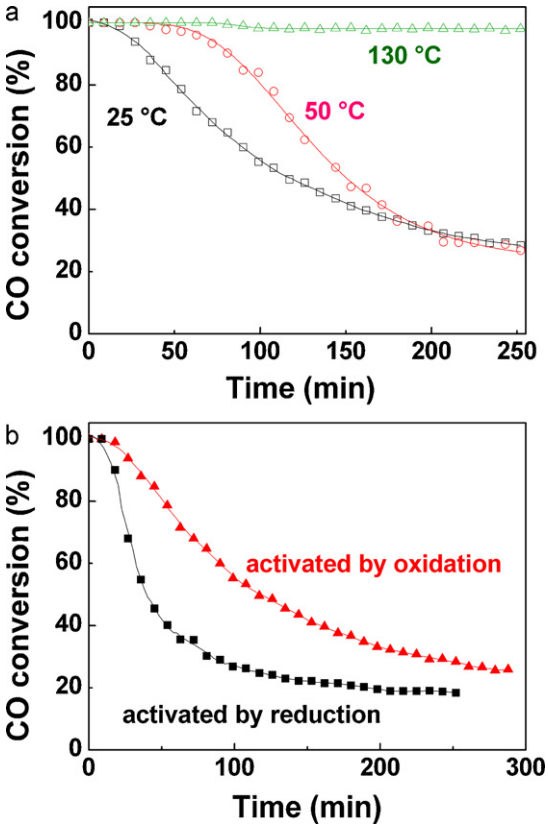

Fig. 2. (a) Influence of the reaction temperature on CO conversion over 5.1%Au/HMS–Fe sample pre-treated by oxidation; (b) influence of the pre-treatment (oxidation versus reduction) on CO oxidation at 25 °C over 5.1%Au/HMS–Fe catalyst.

The next step consisted in the evaluation of performance of pre-treated catalysts. Fig. 1(a) and (b) shows the activity of catalysts activated by oxidation and reduction, respectively. Both figures also include the activity profile of the Au-free HMS–Fe substrate with the purpose of revealing possible contributions of the support to overall CO oxidation activity. As shown in Fig. 1(a), the support activity is poor and only reached 20% at reaction temperature of 400 °C. For the catalysts with high Au loading (>2.1 wt%), the pre-treatment by oxidation resulted in an enhancement of activity whereas the catalysts with a low Au loading (0.4 and 1.2 wt%) showed low activity at temperatures below 200 °C (total CO conversion was reached at temperature of 300 and 250 °C, respectively). In the case of 2.1%Au/HMS–Fe sample, this presented an 82% conversion of CO at room temperature, then CO conversion decreased to 40%, while a further increase of reaction temperature resulted in an increase of CO conversion, reaching 100% of CO conversion above of 180 °C. The best catalytic response was observed with 3.1%Au/HMS–Fe and 5.1%Au/HMS–Fe catalysts which exhibited CO conversion levels of 100% at room temperature. A slight decrease in CO conversion was found in both catalysts upon increasing reaction temperature from 25 to 80 °C. At temperatures above 80 °C the CO conversion increased again to 100%. It is worth noting that both catalysts with high Au-loading (3.1 and 5.1 wt%) showed a similar catalytic behaviour (Fig. 1(b)), which contrasts with other gold catalyst prepared by using non-structured substrates whose activity drops upon increasing metal loading [35].

Important changes in CO conversion profiles were noted when the catalysts were reduced prior to reaction tests (Fig. 1(b)). All reduced catalysts presented high CO conversion at 25 °C. For the 0.4%Au/HMS–Fe catalyst, the CO conversion begin close to 80%, then decreases sharply up to 20% and finally increase again at higher temperature. The resulting U-shaped activity curve, which has been often called "smile effect", is attributed in the literature to the aging of the catalysts and/or to the catalyst poisoning by surface carbonates [36].

The remarkable enhancement of catalytic performance of reduced gold catalysts even at low gold loading differs strongly from those treated in an oxidizing atmosphere. The "U" shaped activity pattern observed for reduced catalysts suggests that this treatment promotes changes in Au species that turn out it more active. In addition to this, it is also apparent that, despite the gold species being more active after the reduction treatment they are also susceptible to losing activity rapidly, as observed in Fig. 1(b). The activity profiles displayed in this figure suggest that saturation of active sites by adsorption of a compound takes place, as it was proposed by Margitfalvi et al. [36], rather than an activation/deactivation of gold active sites due to temperature changes. To test this hypothesis, the CO oxidation reaction was conducted at various temperatures on the 5.1%Au/HMS–Fe catalyst. This catalyst was chosen since the drop in activity in both oxidative and reductive pretreatments was less marked than in the other catalysts. Fig. 2(a) shows the CO conversion versus the time on-stream (*TOS*) at different reaction temperatures for the oxidized 5.1%Au/HMS–Fe catalyst. It can be observed that the stability of this catalyst diminished when the reactor operated at low temperature, undergoing a very fast deactivation at 25 °C. As the temperature of the reactor increases the stability of catalyst increases too, showing at 130 °C almost a 100% of CO conversion during the entire reaction test. The stability of reduced 5.1%Au/HMS–Fe catalyst was also tested in the target reaction at 25 °C (Fig. 2(b)). As can be seen in Fig. 2(b), the drop in activity for catalyst pre-treated by reduction is much more pronounced than that observed in the case of the catalyst pre-treated by oxidation, and also reached a lower CO conversion at the end of the test. From the results of Fig. 2(b), it can be inferred that although the catalyst reduction leads to more active catalysts, the nature of the active sites makes them also more

vulnerable to be deactivated under the reaction stream. This fact is in agreement with the results shown in Fig. 1(b) in which a prominent "U" shape profile is observed. The results of Fig. 2(a) clearly show that the drop in CO conversion observed during the temperature-programmed reaction (Fig. 1(b)) is due to saturation of active sites by the strong adsorption of some species. It is unlikely that during reaction at 25 °C the sintering of gold particles can occur even considering the high exothermicity of the reaction. This idea was supported in this study by DRIFTS analysis of co-adsorption of both CO and O_2 of the surface of 5.1%Au/HMS–Fe sample pretreated by oxidation and reduction (*vide infra*) suggesting that during the course of reaction carbonates are accumulated on the catalyst surface blocking the active sites and then deactivating the catalysts.

On the other hand, the beneficial effect shown for oxidized or reduced catalysts compared to the fresh ones has been often attributed to the development of the active species, where removal of residual chloride (derived from gold precursor) could have an important role [37,38]. Also, the difference in the observed conversion with and without treatment has been associated with modification of gold species, promoted by gold migrations to the support surface [39]. Some studies suggest that catalysts reduced prior to reaction are more effective toward CO oxidation than those oxidized, because reduction promotes changes of gold species toward cationic or metallic state [40]. It has been also suggested that a reduction treatment of the catalyst just before the CO oxidation reaction eliminates dissolved oxygen, being the activity occasionally improved [1]. Nevertheless, there is big uncertainty yet about the factual nature of gold active species, because crucial contributions of the catalyst support are able to enhance oxygen transfer, as in the case of reducible metallic oxides (i.e. CeO_2, TiO_2, Fe_2O_3, Mn_2O_3, etc.), may occur [10,41,42]. Thus, considering that Fe_2O_3 is an active support due to its capability to provide reactive oxygen [41], a possible explanation of the activity enhancement observed for the reduced Au/HMS–Fe systems is that the introduction of a trivalent cation in the silica network generated a positive charge deficit resulting in the formation of anionic vacancies able of activating oxygen, such as it was proposed previously [41,42]. This may result in a stoichiometric reaction at room temperature with adsorbed oxygen suboxides and therefore the reduction pretreatment would influence the catalytic activity and stability at room temperature. Another possibility arises from the interface of Au particles and iron like-oxide species partially reduced, which may act in the same way above described. This could explain also why the catalytic activity increases as the Au-loading in our catalysts increases too.

3.2. Catalyst characterization

Chemical analysis revealed that Au content of Au/HMS–Fe catalysts was close to their nominal Au loading (Table 1). The textural properties of the fresh catalysts were evaluated from the N_2 adsorption–desorption isotherms at 196 °C. The specific area (S_{BET}) of the pure HMS–Fe material and fresh Au/HMS–Fe catalysts are summarized in Table 1. From this table, the S_{BET} decreases after Au incorporation onto HMS–Fe material. The S_{BET} of all catalysts was relatively high (in range 469–721 m^2/g). In order to evaluate the influence of Au loading on the Au species location inside the support structure, the normalized S_{BET} (see Section 2) was calculated. For the catalyst with a low Au loading (0.4, 1.2 and 2.0 wt%), the NS_{BET} values were close to 1 indicating the presence of Au species on the support surface. On the contrary, both catalysts with high Au loading (3.1 and 5.1 wt%) show the NS_{BET} of 0.7 indicating the presence of Au species on the support surface as well as their location within the porous structure of the HMS–Fe support.

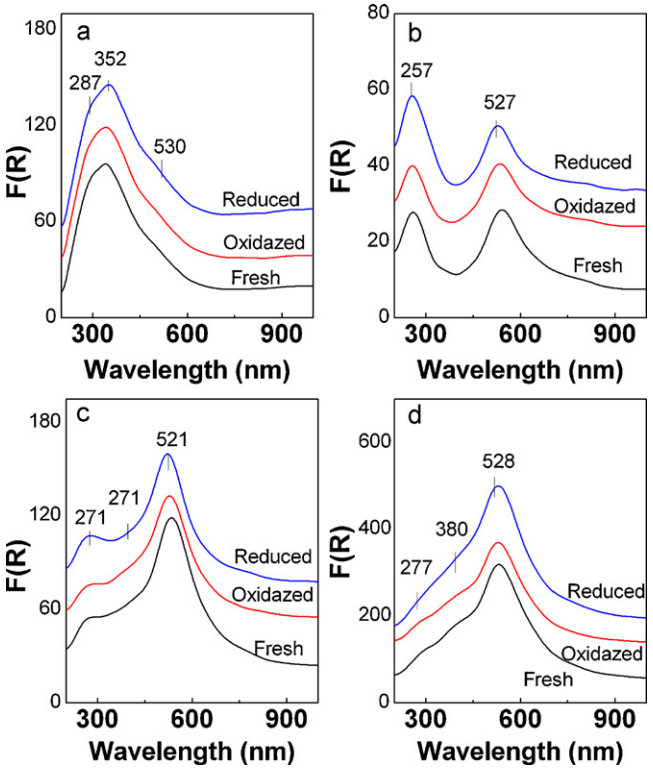

Fig. 3. UV–vis spectra of the pure HMS–Fe substrate and Au/HMS–Fe catalysts before and after pretretments by oxidation (400 °C, 1 h) and reduction (300 °C, 0.5 h). (a) HMS–Fe, (b) 0.4%Au/HMS–Fe, (c) 2.1%Au/HMS–Fe, and (d) 5.1%Au/HMS–Fe.

3.2.1. X-ray diffraction (XRD)

The hexagonal arrangement of HMS–Fe material before and after Au loading was confirmed previously by us via both the low-angle XRD and HRTEM [43]. The high-angle XRD patterns of the calcined Au/HMS–Fe catalysts (not shown here) show four peaks identified at around 38°, 45°, 65° and 78°, which correspond respectively to the planes (1 1 1), (2 0 0), (2 2 0), and (3 1 1) of gold. This observation points out to the presence of a high amount of gold in metallic state [44–46]. The intensity of diffraction lines also increases upon increasing gold loading. The crystalline phase seems to be formed due to sintering of gold crystallites and to the reduction of cationic gold during calcination in static air, such as it has been reported by other authors [12]. Furthermore, the presence of a non-reducible oxide such as silicon dioxide and a reducible oxide such as iron oxide compounds may be decisive for the stabilization of metallic gold particles [47]. XRD diffraction does not show any diffraction lines belonging to Fe_xO_y moieties indicating that either they are amorphous or form crystals smaller than 4 nm, which is the limit of the XRD technique detection. For all catalysts, the Au^0 crystal size, estimated by applying the Debye–Scherrer equation to the XRD line at $2\theta = 38.2°$, was in range 3.3–4.5 nm. The spent catalysts do not show important changes in the particle size of gold even after being used several times for on-stream experiments of 4 h at 130 °C (data not shown here).

3.2.2. UV–vis characterization

The changes in gold species upon subjecting catalysts to different treatments were evaluated using the same in situ pretreatments (UV–vis chamber) than those performed prior to catalyst testing. Fig. 3(a)–(d) shows the electronic UV–vis spectra for the fresh catalysts and after treatment in reducing and oxidizing atmosphere. The spectrum of the reference HMS–Fe substrate is also included for comparison. As can be seen in Fig. 3(a), the HMS–Fe substrate shows a wide band at 287 nm which can be

attributed to a charge transfer from ligand-to-metal which is associated with the incorporation of Fe^{+3} species within the frame of HMS structure in a tetrahedral geometry [48,49]. The bands centered at 352 and 530 nm are associated with the aggregation of iron oxides species in a modified tetrahedral geometry (inside the frame of HMS) and with iron oxides species outside the frame, respectively [48,49]. A slight increase in intensity of the band at 352 nm takes place in the substrate pre-treated under a reducing atmosphere (Fig. 3(a)). This increase could be due to iron oxide species that reduce to FeO_x by partial removal of oxygen ligands. In Fig. 3(b)–(d), the UV–vis spectra of the Au/HMS–Fe catalysts are compared before and after oxidation or reduction. In order to avoid interference of the charge transfer (CT) effect, the spectrum of the pre-treated support by oxidation or reduction (Fig. 3(a)) was subtracted from those of gold catalyst pre-treated by the same method. This is a rough approach because the bands corresponding to FeO_x (352 nm) and Fe_xO_y (530 nm) species are affected by the catalyst treatments, however due that the contribution of Au bands in the spectra is high we thought that it is possible to associate qualitatively the observed changes in the spectra only to the change of Au species. In Fig. 3(b)–(d) the fresh and pre-pretreated gold catalysts shown the bands corresponding to: (i), the plasmon resonance assigned to Au^0 at 520–560 nm; (ii), partial charged gold clusters ($Au^{\delta+}$): 300–390 nm; and (iii), gold cations (Au^{3+}) at 260–295 nm in good agreement with literature [36,44,45]. The catalysts containing gold loadings below or equal to 3% (w/w) had the plasmon resonance band assigned to Au^0 species diminished in intensity after the pre-treatments, independently if the pre-treatment was in oxidative or reductive atmosphere (Fig. 3(b) and (c)). 5.1%Au/HMS–Fe catalyst (Fig. 3(d)) exhibits a different behaviour because the intensity of the band of Au^0 diminished when the catalyst was treated under oxidative atmosphere. An increase of the band at 528 nm after 5.1%Au/HMS–Fe catalyst reduction can be reasonably ascribed to gold particles with a more marked metallic character promoted by partial sintering of gold crystallites due to the reductive atmosphere. It is observed from the UV–vis spectra of the catalysts that the decrease of the intensity of the Au^0 band is associated with the simultaneous increase in cationic species. Even though the 5.1%Au/HMS–Fe catalyst was treated under reductive atmosphere, and shows a broad Au^0 band, the presence of UV–vis bands for cationic species that are overlapped with the plasmon resonance band could be observed. This is a strong indication that cationic species are responsible of the high activity showed by catalysts subjected to reduction treatment prior to perform the CO oxidation reaction, because all of them showed a high activity at 25 °C at the beginning of the reaction tests (see Fig. 1(b)). The evidence that cationic gold species are responsible of the high activity has been proposed before for gold catalysts supported in CeO_2, SiO_2, and Ti-SBA-15 among others model catalysts [17,50,51].

3.2.3. XPS characterization

The chemical states of gold on the surface of calcined catalysts were determined by photoelectron spectroscopy. Fig. 4(a) shows the XPS spectrum of all Au/HMS–Fe samples in the Au 4f region archived at pass energy value of 20 eV. In this region each gold species shows two peaks corresponding to Au $4f_{7/2}$ and Au $4f_{5/2}$ transitions (a doublet with spin-orbit splitting of 3.6 eV). In the following, the values of BE will reference the Au $4f_{7/2}$ peak only. For all samples, the peaks Au $4f_{7/2}$ and Au $4f_{5/2}$ transitions were symmetric and full width at half-maximum (FWHM) values of the Au $4f_{7/2}$ peak in range 2.4–2.7 eV. Table 2 summarizes the values of binding energies (BEs), FWHM and Au/Si and Fe/Si atomic ratios obtained on all the tested samples. Regardless of Au loading, all catalysts show this peak at binding energy (BE) value of bulk Au (84.1 ± 0.1 eV) [34–36]. No evident change in the peak maxima is observed with an increase of Au loading of the catalysts. Thus, the spectra of the

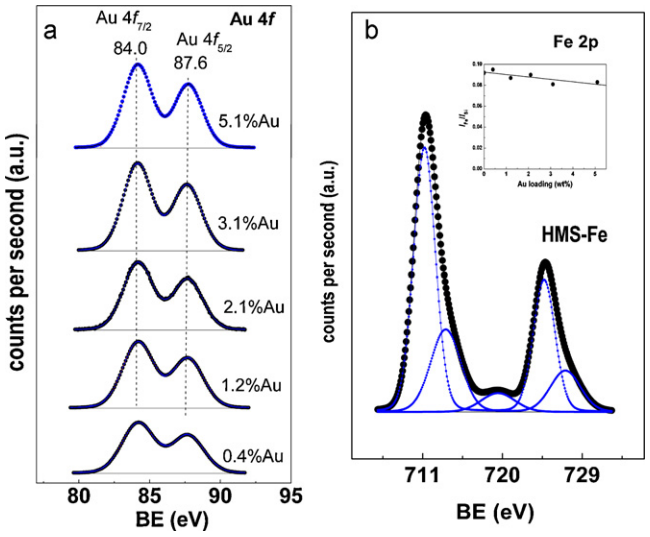

Fig. 4. (a) Au 4f core-level spectra of the calcined Au/HMS–Fe catalysts, and (b) Fe 2p core level spectra of the pure HMS–Fe substrate and Fe/Si atomic ratio versus Au loading.

Au $4f_{7/2,5/2}$ levels do not show indications of the presence of more than one oxidation state for gold in the freshly calcined catalysts. Moreover, the Au 4f core-level spectra of the 3.1%Au/HMS–Fe and 5.1%Au/HMS–Fe catalysts does not show any shift of the Au $4f_{7/2}$ peak at 84.1 ± 0.1 eV, suggesting that the Au particle size distribution could be the same for both catalysts [52]. The XPS analysis did not evidence the presence of Au^+ species in the calcined catalyst, nor in those subjected to oxidizing or reducing treatments (Table 2). However, a direct evidence of AuO^-, AuO_2 and $AuOH^-$ ion clusters on supported Au catalysts has been recently reported by a time-of-flight secondary-ion mass-spectroscopy (TOF-SIMS), whereas the XPS of the same samples did not detected those species [53]. Furthermore, as can be expected, the Au/Si atomic surface ratio for fresh 5.1%Au/HMS–Fe was greater than for the corresponding 3.1%Au/HMS–Fe counterpart, reflecting the differences in gold loading in both catalysts.

In order to get information on the state of iron species in the HMS–Fe support, the Fe 2p region of gold catalysts has been analyzed. As example, the Fe 2p core level of the pure HMS–Fe material is shown in Fig. 4(b). The Fe 2p pattern of all investigated Au-containing samples showed a large peak at a BE of 710.9–711.2 eV together with the presence of satellite peaks at higher BE characteristic of Fe^{3+} species [30]. The inset in Fig. 4(b) shows the Fe/Si atomic ratio versus the Au loading of gold catalysts. As seen in this figure, the surface exposure of iron species decreased with an increase of the Au loading of the catalysts. As seen in Table 2, the pre-treatment of 5.1%Au/HMS–Fe sample by oxidation or reduction did not change the iron species surface exposure and their oxidation state. This

Table 2
Binding energies (eV) of core electrons and surface atomic ratios of the pure HMS–Fe material and fresh Au/HMS–Fe samples.

Catalyst	Au $4f_{7/2}$ (FWHM)	Fe $2p_{3/2}$	Au/Si at	Fe/Si at
HMS–Fe	–	710.9	–	0.092
0.4%Au/HMS–Fe	84.2 (2.5)	710.9	0.0007	0.095
1.2%Au/HMS–Fe	84.1 (2.6)	711.0	0.0014	0.087
2.0%Au/HMS–Fe	84.1 (2.5)	710.9	0.0024	0.090
3.1%Au/HMS–Fe	84.0 (2.4)	711.2	0.0042	0.081
5.1%Au/HMS–Fe	84.0 (2.5)	711.2	0.0072	0.083
5.1%Au/HMS–Fe (oxi)[a]	84.2 (2.1)	711.1	0.0076	0.082
5.1%Au/HMS–Fe (red)[b]	84.3 (2.4)	711.1	0.0075	0.082

[a] After oxidation in air at 400 °C for 1 h.
[b] After reduction in 10% H_2/N_2 mixture at 300 °C for 0.5.

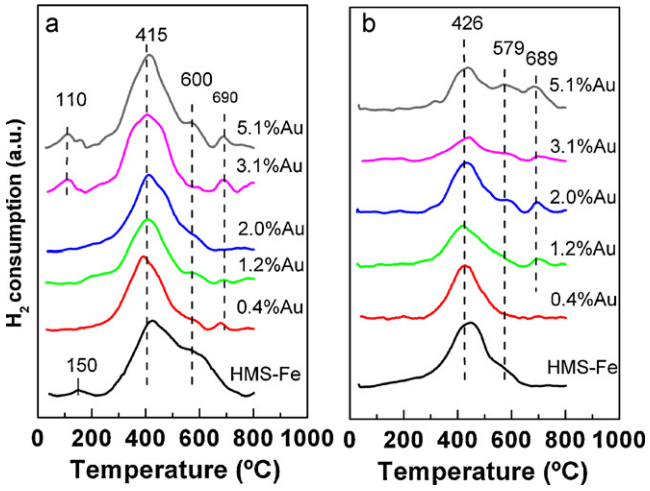

Fig. 5. H_2-TPR patterns for Au/HMS–Fe catalysts and HMS–Fe substrate treated in situ: (a) oxidized and (b) reduced samples.

result reinforces the idea that the interface between Au particles and iron like-oxides species could play a key role in the activity of this kind of model catalysts, because the activity increases as the Au loading increases too.

3.2.4. Temperature-programmed reduction (H_2-TPR)

The reducibility of pure HMS–Fe support and Au/HMS–Fe catalysts pre-treated using oxidative and reductive atmosphere was examined by H_2-TPR analysis (Fig. 5(a) and (b), respectively). For all H_2-TPR profiles, the hydrogen consumption was normalized considering the catalyst weight and their respective surface area (see Table 1) considering this as the surface exposed to reaction. As can be seen from Fig. 5(a), the pure HMS–Fe support and all Au/HMS–Fe catalysts show two reduction peaks at 415 and 600 °C which are attributed to reduction of Fe_2O_3 and Fe_3O_4 species located inside the porous network, respectively [54]. Additionally, gold catalysts shown a peak at 690 °C attributed to further reduction of Fe^{2+} species to metallic iron [45]. There is not an evident contribution of gold species neither to the peak temperature nor to hydrogen consumption. A small reduction peak arise in 3.1%Au/HMS–Fe and 5.1%Au/HMS–Fe catalysts at 110 °C which is difficult to explain, however some researchers have observed a peak at low temperature and have attributed this to the reduction of oxidized gold species [44,55,56].

Fig. 5(b) shows the H_2-TPR patterns of reduced catalysts and Au-free HMS–Fe support. The reduction peak at around 426 °C due to reduction of Fe(III) species is observed clearly for the support and all the gold catalysts. It is interesting that the H_2-TPR profile area for the oxidized support is much higher than for the reduced one which should means that the reduction pre-treatment partially reduces iron like-oxides. On increasing the gold content the H_2-TPR profile area decreases even more compared with Au-free HMS–Fe support, which suggest that Au presence favors the reducibility of iron oxide-like (Fe_xO_y) species by performing a pre-treatment on reductive atmosphere. It is known that gold has a limited capacity to dissociate H_2 molecules due to the completely filled electronic *d*-band. However, the hydrogen could be dissociatively adsorbed on supported Au atoms, but such adsorption and dissociation is limited to the gold atoms on corner and edge positions [57]. Indeed, the adsorption of H_2 on gold species of Au/HMS–Fe sample was confirmed by us previously via H_2-TPD measurements [43]. This result suggests also that the interface between Au particles and iron oxide-like species is determinant for attaining good catalytic activity. Also, it cannot be discarded that molecular hydrogen adsorbs and dissociates on the under-coordinated Si atoms of the support, such as it was observed previously [58], and contribute (probably in small extent) to iron oxide-like species reduction.

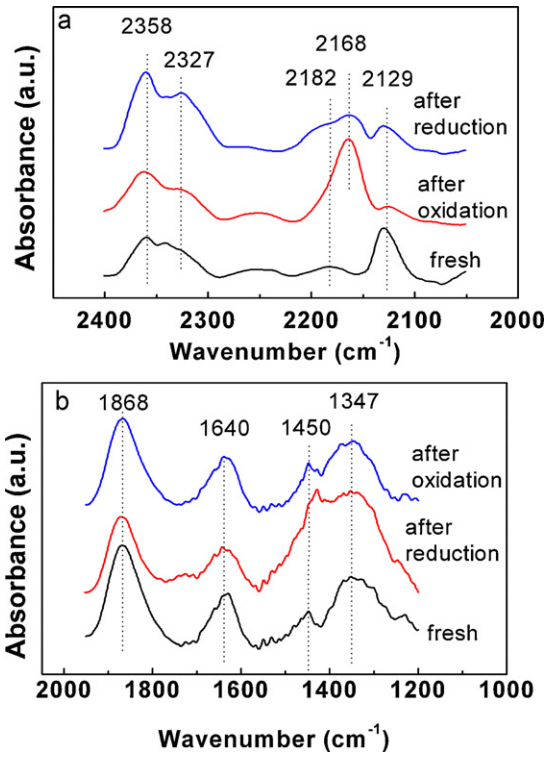

Fig. 6. DRIFTS spectra during CO oxidation at room temperature (4% CO in air for 30 min) for 5.1%Au/HMS–Fe catalyst before and after pre-treatments by oxidation (air; 400 °C, 1 h) and reduction (H_2; 300 °C, 0.5 h). (a) Carbonyl and (b) carbonate sections.

3.2.5. DRIFT spectroscopic measurements

DRIFTS study was used to monitor the possible active sites of oxidized and reduced 5.1%Au/HMS–Fe catalyst for the CO oxidation reaction (chosen as model by its high activity). Fig. 6(a) and (b) shows the carbonyl and carbonates sections after saturation of its surface with CO and O_2 molecules (4% CO in air for 30 min), respectively. Considering the carbonyl region, absorption bands at 2358, 2182, 2168 and 2129 cm^{-1} are observed. An intense band at 2358 cm^{-1} is due to adsorbed CO_2 adsorbed on acid sites of the support surface [41]. The presence of this band suggests that CO oxidation to CO_2 proceeds with participation of the oxygen species from the support [42]. One might note that reduced catalyst shows a high intensity band indicating a larger support participation in the CO_2 formation. The band at 2182 cm^{-1} has also been detected on the fresh and reduced sample. The high stability of this band after catalyst reduction suggests that it could be due to the carbonyls adsorbed on isolated Au^+ sites, as it was proposed by Venkov et al. [59], evidencing that, at least, a certain proportion of gold has acquired a cationic character during the hydrogen treatment. The presence of the band at 2129 cm^{-1} suggests the presence of positively charged gold species in the fresh and reduced catalysts [60]. The comparison of the intensities of both bands indicates that oxidized catalyst has a lower amount of Au cationic species than the reduced one, which is in agreement with the results of UV–vis characterization. Similarly to other reports [28,61], the presence of Au^0 species (band around 2100 cm^{-1}) was not detected. Considering the explanation proposed by Costello et al. [61], this is because a weaker Au^0–CO interaction as compared with Au^+–CO interaction. Finally, the band at 2168 cm^{-1} is attributed to the interaction of CO with the hydroxyl groups of the silica [62]. As expected, the oxi-

dized sample showed a larger intensity of this band than fresh and reduced samples indicating the formation of –OH groups during catalyst oxidation.

The catalyst pre-treatment method influenced also the catalyst deactivation behaviour, as deduced from the carbonate section of the DRIFTS spectrum of this catalyst (Fig. 6(b)). The introduction of the 4% CO + air mixture at room temperature for 0.5 h, lead to the appearance of bands at 1347 cm^{-1} and 1240 cm^{-1} due to monodentate carbonates together with a band at 1450 cm^{-1}, indicative of bidentate bridging [28]. The same species were formed on the oxidized and reduced catalysts, although lower formation was obtained with the latter treatment.

3.3. Proposal for scheme of CO oxidation reaction with use of Au–HMS–Fe

Due to a relatively low Au loading (0.4–5.1 wt%) and a large specific surface area of all catalysts (469–750 m^2/g), the catalyst activity was not influenced by the specific surface area. Before going any further into activity results, it is important to first understand the influence of Au loading on the type of gold species formed on surface of Au/HMS–Fe catalysts before and after the catalyst pre-treatment by oxidation or reduction. In this study, both UV–vis and DRIFTS spectra suggest that the reduction of the catalyst led to formation of a larger amount of Au cationic species, probably in the form of $Au(OH)_3$ or Au(OH) located at the perimeter interfaces at the conditions where water is present [28]. Moreover, the UV–vis spectra indicated that the oxidation treatment leads to a decrease in the amount Au^0 particles, and therefore the presence of gold oxide particles cannot be discarded. However, the formation of an important fraction of cationic species arises from both treatments (reduction and oxidation), being more marked in the case of catalysts having less than 3% (w/w) of gold loading. The best treatment to achieve good activity was the reduction, showing high activity at 25 °C. The in situ UV–vis and DRIFTS spectra showed also an important formation of cationic sites under this treatment. Accordingly, it can be inferred that cationic sites are mainly responsible for the low temperature activity; this can explain why the catalysts even with the lowest gold content show a high activity at 25 °C. The support participation in the reaction mechanism is highly possible because the introduction of a trivalent cation in the silica network generated a positive charge deficit resulting in the formation of anionic vacancies able of activating oxygen, as it was proposed previously [41,42]. Moreover, the enhancement of reduction promoted by Au presence observed in H_2-TPR profiles indicates that an interface between Au particles and iron oxide-like species plays an important role. This may result in a direct interaction of CO molecules with adsorbed oxygen suboxides, and therefore the reduction pre-treatment would influence the catalytic activity and stability of these species at room temperature.

Considering the catalyst stability tests and DRIFTS analysis results, the drop in activity observed for reduced samples at the beginning of the reaction suggests a strong interaction of the active species with the reactants and/or reaction products. On the opposite, better stability was observed for the oxidized catalysts, which indicates that the ability to activate O-atom can be a key step for the CO oxidation reaction. With these observations, we propose that the interface of gold with iron oxide should be available for the dissociation of oxygen molecules, being the iron oxide-like species responsible of keeping the gold in a cationic state (Scheme 1). The scheme proposed is in agreement with those suggested by Haruta et al. for Au/TiO_2 catalyst [63]. This scheme also explains the observed sharp drop in activity when the catalysts are treated under a reductive atmosphere. If the iron oxide is not stoichometric, such as it is expected to occur in the reduced catalysts, the oxide will tend to get the necessary oxygen in order to be stabilized in the reaction atmosphere. This could provoke incomplete oxygen dissociation, and perhaps deactivate the attack of partially dissociated oxygen to CO molecules, making stronger the molecule adsorption of the formed intermediates (likely carbonates), whose formation was confirmed by DRIFTS study on the co-adsorption of both CO and O_2 onto oxidized and reduced 5.1%Au/HMS–Fe catalyst.

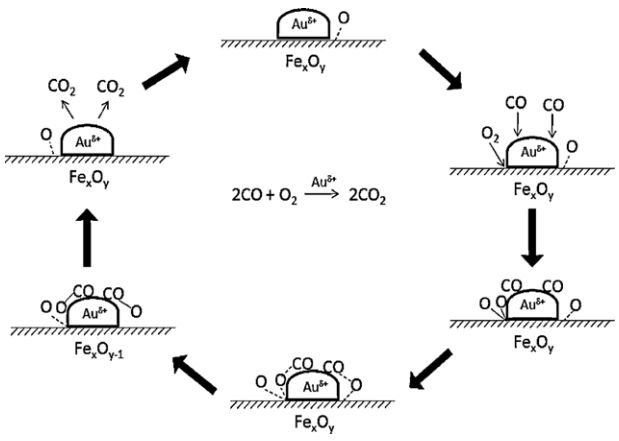

Scheme 1. Reaction scheme for total CO oxidation over Au/HMS–Fe catalysts.

4. Conclusions

In this study, gold catalysts supported on iron-loaded HMS were tested in the CO oxidation reaction. Activity was found to be a function of the gold content and the pre-treatment process of the catalysts. It was observed that the metallic character of gold increases in parallel with the metal content. Oxidation and reduction treatments lead to formation of cationic gold species, which resulted in higher activity and a complete conversion of CO for the high metal loading catalysts (3 and 5.1%, w/w) in the temperature interval explored (room temperature up to 400 °C). Furthermore, the reduction treatment of the catalysts with a gas mixture with 10% (v/v) of H_2 resulted to be most effective for catalysts activation, reaching high CO conversion at 25 °C even with the low metal loading. However the reduced catalysts are more susceptible to be deactivated rapidly, presumably because the extraction of O-atoms from the iron oxide during reduction treatment results in a non-stoichiometric oxide (FeO_x). This iron oxide-like species will try to diminish the oxygen deficiency under reaction conditions, provoking that the intermediate carbonate species being strongly adsorbed, blocking the Au-iron oxide-like perimeter for further reaction molecules. The characterization results suggest that CO oxidation reaction might well take place at the Au-iron interface.

Acknowledgements

A.M.H. acknowledge the financial support of PROMEP (103-5/07/2523 and 103-5/08/4801) and CONACYT (Project: 82880) R.E. R-G. gratefully acknowledges a graduate scholarship from CONACYT. T.A.Z. acknowledges financial support from the CNyN-UNAM. B.P. acknowledges financial support from the Spanish Ministry of Science and Innovation (ENE2007-67533-C02-01) and the Comunidad de Madrid (S2009/ENE-1743). Thanks are due to Prof. J.L.G. Fierro for results discussion and Mrs. C.V. Loricera for performing DRIFTS measurements.

References

[1] G.C. Bond, Gold Bull. 41 (3) (2008) 235–241.
[2] G.C. Bond, P.A. Sermon, Gold Bull. 6 (4) (1973) 102–105.
[3] P.A. Sermon, Gold Bull. 9 (4) (1976) 129–131.

[4] M. Haruta, T. Kobayashi, H. Sano, N. Yamada, Chem. Lett. (1987) 405–408.
[5] G.C. Bond, D.T. Thompson, Catal. Rev. Sci. Eng. 41 (1999) 319–388.
[6] (a) G.J. Hutchings, Catal. Today 72 (2002) 11–17;
(b) G.J. Hutchings, Catal. Today 100 (2005) 55–61.
[7] G.R. Bamwenda, S. Tsubota, T. Nakamura, M. Haruta, Catal. Lett. 44 (1997) 83–87.
[8] M. Bowker, A. Nuhu, J. Soares, Catal. Today 122 (2007) 245–247.
[9] G. Glaspell, H.M.A. Hassan, A. Elzatahry, V. Abdalsayed, M. Samy El-Shall, Top. Catal. 47 (2008) 22–31.
[10] M. Haruta, Catal. Sur. Jpn. 1 (1997) 61–73.
[11] M. Valden, S. Paka, X. Lai, D.W. Goodman, Catal. Lett. 56 (1998) 7–10.
[12] G.C. Bond, D.T. Thompson, Gold Bull. 33 (2) (2000) 41–51.
[13] F. Romero-Sarria, L.M.T. Martinez, M.A. Centeno, J.A. Odriozola, J. Phys. Chem. C 111 (2007) 14469–14475.
[14] D. Horváth, L. Toth, L. Guczi, Catal. Lett. 67 (2000) 117–128.
[15] A.C. Gluhoi, X. Tang, P. Marginean, B.E. Nieuwenhuys, Top. Catal. 39 (2006) 1–2.
[16] E.D. Park, J.S. Lee, J. Catal. 186 (1999) 1–11.
[17] N.A. Hodge, C.J. Kiely, R. Whyman, M.R.H. Siddiqui, G.J. Hutchings, Q.A. Pankhurst, F.E. Wagner, R.R. Rajaram, S.E. Golunski, Catal. Today 72 (2002) 133–144.
[18] J. Guzman, B. Gates, J. Phys. Chem. B 106 (2002) 7659–7665.
[19] L. Guczi, D. Horváth, Z. Pászti, G. Petõ, Catal. Today 72 (2002) 101–105.
[20] A. Simakov, I. Tuzovskaya, A. Pestriyakov, N. Bogdanchikova, V. Gurin, M. Avalos, M.H. Farías, Appl. Catal. A: Gen. 331 (2007) 121–128.
[21] K. Nakagawa, K. Anzai, N. Matsui, N. Ikenaga, T. Suzuki, Y. Teng, T. Kobayashi, M. Haruta, Catal. Lett. 51 (1998) 163–167.
[22] G.C. Bond, Gold Bull. 31 (1998) 109–110.
[23] H. Zhu, C. Liang, W. Yan, S.H. Overbury, S. Dai, J. Phys. Chem. B 110 (2006) 10842–10848.
[24] Z. Ma, S. Brown, J.Y. Howe, S.H. Overbury, S. Dai, J. Phys. Chem. C 112 (2008) 9448–9457.
[25] P.T. Tanev, T.J. Pinnavaia, Chem. Mater. 8 (1996) 2068–2079.
[26] W. Zhang, M. Fröba, J. Wang, P.T. Tanev, J. Wong, T.J. Pinnavaia, J. Am. Chem. Soc. 118 (1996) 9164–9171.
[27] T.A. Zepeda, Appl. Catal. A: Gen. 347 (2008) 148–161.
[28] M.C. Raphulu, J. McPherson, E. van der Lingen, J.A. Anderson, M.S. Scurrell, Gold Bull. 43 (4) (2010) 334–344.
[29] G.C. Bond, C. Louis, D.T. Thompson, Catalysis by Gold , Imperial College Press, London, 2006.
[30] A.M. Visco, F. Neri, G. Neri, A. Donato, C. Milone, S. Galvano, Phys. Chem. Chem. Phys. 1 (1999) 2869–2873.
[31] B. Schumacher, Y. Denkowitz, V. Plzak, M. Kinne, R.J. Behm, J. Catal. 224 (2004) 449–462.
[32] N.M. Schubert, A. Venugopal, M.J. Kalich, V. Plazk, R.J. Behm, J. Catal. 222 (2004) 32–40.
[33] T.A. Ntho, J.A. Anderson, M.S. Scurrell, J. Catal. 261 (2009) 94–100.
[34] P. Castaño, T.A. Zepeda, B. Pawelec, M. Makkee, J.L.G. Fierro, J. Catal. 267 (2009) 30–39.
[35] L. Delannoy, N. El Hassan, A. Musi, N.N. Le To, J.-M. Krafft, C. Louis, J. Phys. Chem. B 110 (2006) 22471–22478.
[36] J.L. Margitfalvi, A. Fási, M. Hegedus, F. Lónyi, S. Gobölös, N. Bogdanchikova, Catal. Today 72 (2002) 157–169.
[37] F. Arena, P. Famulari, N. Interdonato, G. Bonura, F. Frusteri, L. Spadaro, Catal. Today 116 (2006) 384.
[38] A. Hugon, N. El Kolli, C. Louis, J. Catal. 274 (2010) 239–250.
[39] Y.M. Kang, B.Z. Wan, Catal. Today 26 (1995) 59–69.
[40] W. Deng, C. Carpenter, N. Yi, M. Flytzani-Stephanopoulos, Top. Catal. 44 (1–2) (2007) 199–208.
[41] M.I. Domínguez, F. Romero-Sarria, M.A. Centeno, J.A. Odrizola, Appl. Catal. B: Environ. 87 (2009) 245–251.
[42] R. Romero-Sarria, A. Penkova, L.M.T. Martinez, M.A. Centeno, K. Hadjiivanov, J.A. Odriozola, Appl. Catal. B: Environ. 84 (2008) 119–124.
[43] T.A. Zepeda, A. Martinez-Hernández, R. Guil-López, B. Pawelec, Appl. Catal. B: Environ. 100 (2010) 450–462.
[44] A.C. Gluhoi, X. Tang, P. Marginean, B.E. Nieuwenhuys, Top. Catal. 39 (1–2) (2006) 101–110.
[45] W. Gac, J. Goworek, G. Wójcik, L. Kepinski, Adsorption 14 (2008) 247–256.
[46] S. Peng, Y. Lee, C. Wang, H. Yin, S. Dai, S. Sun, Nano. Res. 1 (2008) 229–234.
[47] W. Yan, S.M. Mahurin, B. Chen, S.H. Overbury, S. Dai, J. Phys. Chem. B 109 (2005) 15489–15496.
[48] Y. Wang, Q. Zhang, T. Shishido, K. Takehira, J. Catal. 209 (2002) 186–196.
[49] H. Liu, G. Lu, Y. Guo, Y. Guo, J. Wang, Microporous Mesoporous Mater. 108 (2008) 56–64.
[50] C.L. Peza-Ledesma, L. Escamilla-Perea, R. Nava, B. Pawelec, J.L.G. Fierro, Appl. Catal. A: Gen. 375 (2010) 37–48.
[51] M.P. Casaletto, A. Longo, A.M. Venezia, A. Martorana, A. Prestianni, Appl. Catal. A: Gen. 302 (2006) 309–316.
[52] T. Diemant, Z. Zhao, H. Rauscher, J. Bansmann, R.J. Behm, Top. Catal. 44 (2007) 83–93.
[53] L. Fu, N.Q. Wu, J.H. Yang, F. Qu, D.L. Johnson, M.C. Kung, H.H. Kung, V.P. Dravid, J. Phys. Chem. B 109 (2005) 3704–3706.
[54] X. Wang, Y.C. Xie, React. Kinet. Catal. Lett. 72 (2001) 229–237.
[55] I. Tuzovskaya, N. Bogdanchikova, A. Simakov, V. Gurin, A. Pestryakov, M. Avalos, M.H. Farías, Chem. Phys. 338 (2007) 23–32.
[56] H. Zhengping, A. Lidun, W. Hongli, Sci. China (Ser. B) 44 (2001) 596–605.
[57] L. Bus, J.T. Miller, J.A. van Bokhoven, J. Phys. Chem. B 109 (2005) 14581–14587.
[58] G. Zhao, W. Zhang, J. Sun, X. Shen, Y. Wang, J. Mol. Struct.: Theochem. 941 (2010) 71–77.
[59] Tz. Venkov, Hr. Klimev, M.A. Centeno, J.A. Odriozola, K. Hadjiivanov, Catal. Commun. 7 (2006) 308–313.
[60] F. Boccuzzi, A. Chiorino, M. Manzoli, P. Lu, T. Akita, S. Ichikawa, M. Haruta, J. Catal. 202 (2001) 256–267.
[61] C.K. Costello, M.C. Kung, H.-S. Oh, Y. Wang, H.H. Kung, Appl. Catal. A: Gen. 232 (2002) 159–168.
[62] T.P. Beebe, P. Gelin, J.T. Yates, Surf. Sci. 148 (1984) 526–550.
[63] M. Haruta, Cattech 6 (2002) 102–115.